Received: 2 December 2018 | Accepted: 8 August 2019

DOI: 10.1111/gcb.14836

PRIMARY RESEARCH ARTICLE

Global Change Biology WILEY

Arctic shrub colonization lagged peak postglacial warmth: Molecular evidence in lake sediment from Arctic Canada

Sarah E. Crump[1,2] | Gifford H. Miller[1,3] | Matthew Power[3] | Julio Sepúlveda[1,2] | Nadia Dildar[1,2] | Megan Coghlan[3] | Michael Bunce[3]

[1]Institute of Arctic and Alpine Research and Department of Geological Sciences, University of Colorado Boulder, Boulder, CO, USA

[2]Organic Geochemistry Laboratory, University of Colorado Boulder, Boulder, CO, USA

[3]Trace and Environmental DNA (TrEnD) Laboratory, School of Molecular and Life Sciences, Curtin University, Bentley, WA, Australia

Correspondence
Sarah E. Crump, Institute of Arctic and Alpine Research and Department of Geological Sciences, University of Colorado Boulder, Boulder, CO 80303, USA.
Email: sarah.crump@colorado.edu

Funding information
NSF, Grant/Award Number: DGE1144083, BCS1657743 and ARC1737712; National Geographic Society; Geological Society of America; CU Department of Geological Sciences; CU Center for the Study of Origins; INSTAAR

Abstract

Arctic shrubification is an observable consequence of climate change, already resulting in ecological shifts and global-scale climate feedbacks including changes in land surface albedo and enhanced evapotranspiration. However, the rate at which shrubs can colonize previously glaciated terrain in a warming world is largely unknown. Reconstructions of past vegetation dynamics in conjunction with climate records can provide critical insights into shrubification rates and controls on plant migration, but paleoenvironmental reconstructions based on pollen may be biased by the influx of exotic pollen to tundra settings. Here, we reconstruct past plant communities using sedimentary ancient DNA (*sed*aDNA), which has a more local source area than pollen. We additionally reconstruct past temperature variability using bacterial cell membrane lipids (branched glycerol dialkyl glycerol tetraethers) and an aquatic productivity indicator (biogenic silica) to evaluate the relative timing of postglacial ecological and climate changes at a lake on southern Baffin Island, Arctic Canada. The *sed*aDNA record tightly constrains the colonization of dwarf birch (*Betula*, a thermophilous shrub) to 5.9 ± 0.1 ka, ~3 ka after local deglaciation as determined by cosmogenic ^{10}Be moraine dating and >2 ka later than *Betula* pollen is recorded in nearby lake sediment. We then assess the paleovegetation history within the context of summer temperature and find that paleotemperatures were highest prior to 6.3 ka, followed by cooling in the centuries preceding *Betula* establishment. Together, these molecular proxies reveal that *Betula* colonization lagged peak summer temperatures, suggesting that inefficient dispersal, rather than climate, may have limited Arctic shrub migration in this region. In addition, these data suggest that pollen-based climate reconstructions from high latitudes, which rely heavily on the presence and abundance of pollen from thermophilous taxa like *Betula*, can be compromised by both exotic pollen fluxes and vegetation migration lags.

KEYWORDS

ancient DNA, Arctic shrubification, deglaciation, dispersal, paleoclimate, paleothermometry, paleovegetation

1 | INTRODUCTION

Rapid summer warming in the Arctic is expected to promote an increase in the biomass, cover, and abundance of deciduous shrubs, as well as the northward migration of shrubline (Myers-Smith et al., 2011). This 'shrubification' response to warming has been confirmed experimentally (Chapin, Shaver, Giblin, Nadelhoffer, & Laundre, 1995; Walker et al., 2006; Zamin & Grogan, 2012), and is already observable both in plot studies (Elmendorf et al., 2012; Tape, Sturm, & Racine, 2006) and via remote sensing (Goetz, Bunn, Fiske, & Houghton, 2005; Ju & Masek, 2016; Myneni, Keeling, Tucker, Asrar, & Nemani, 1997). Increased woody vegetation at high latitudes not only impacts local biodiversity and ecological interactions (Fauchald, Park, Tømmervik, Myneni, & Hausner, 2017; Walker et al., 2006), but also plays an important role in the global climate system by decreasing albedo and increasing atmospheric water vapor (Bonfils et al., 2012; Pearson et al., 2013; Sturm, Douglas, Racine, & Liston, 2005; Swann, Fung, Levis, Bonan, & Doney, 2010). The rate at which shrubification will proceed in the future, however, is largely unknown, meaning that these positive feedbacks on climate warming may not be correctly captured by current earth system models (Pearson et al., 2013).

The rates and patterns of tundra ecosystem change following the last glacial cycle can provide insights into how shrubs move north in a warming world and colonize previously glaciated terrain. Paleorecords based on fossil pollen and plant macrofossils have revealed dramatic biogeographical shifts of Arctic plants in response to repeated Quaternary glacial–interglacial cycles (Birks, 2008; Davis & Shaw, 2001). These traditional paleoecological approaches are compromised in treeless landscapes, however, because of the long-distance wind dispersal of pollen from Arctic shrubs and boreal trees that contribute to the pollen signal (Birks & Birks, 2000; Jacobson & Bradshaw, 1981), and the sparseness of macrofossils in sedimentary records (Anderson-Carpenter et al., 2011). How quickly Arctic vegetation re-colonizes landscapes following deglaciation thus remains an open question. A genetic study of modern Arctic flora pointed to the rapid and repeated postglacial plant colonization of Svalbard, thereby suggesting that shrub establishment in some remote northern regions is limited primarily by climate rather than long-distance dispersal (Alsos et al., 2007). Yet, direct evidence that shrub ranges can rapidly shift in a warming climate to fill an ecological niche, particularly on Arctic islands, is lacking.

In this study, we explore postglacial vegetation patterns at a lake on southern Baffin Island (Nunavut, Canada) in the context of Holocene climate fluctuations. Baffin Island is an ideal setting to test the efficiency of postglacial shrub colonization, as it was completely ice-covered during the Last Glacial and isolated from southern populations of shrubs. We first constrain the timing of local deglaciation by dating a lake-impounding moraine with cosmogenic ^{10}Be and calibrating previously published ^{14}C ages from nearby deglacial raised marine deposits (Figure 1). We then analyze ancient plant DNA from a lake sediment core via *sed*aDNA metabarcoding, a powerful technique for detecting local terrestrial and aquatic plant taxa through time (Alsos et al., 2018; Niemeyer, Epp, Stoof-leichsenring, & Herzschuh, 2016; Parducci et al., 2017; Sjögren et al., 2016). We combine this vegetation record with paleothermometry based on bacterial lipids (branched glycerol dialkyl glycerol tetraethers, brGDGTs; Russell, Hopmans, Loomis, Liang, & Sinninghe, 2018) and an aquatic productivity proxy (biogenic silica, BSi) to evaluate the establishment and subsequent evolution of tundra and aquatic communities through climate fluctuations at one well-characterized site. This novel combination of molecular proxies in a lake sediment core provides a detailed view into postglacial ecosystem development during the insolation-driven warmth of the early Holocene (Holocene Thermal Maximum, HTM), most notably in identifying the colonization timing of the thermophilous shrub *Betula* (dwarf birch).

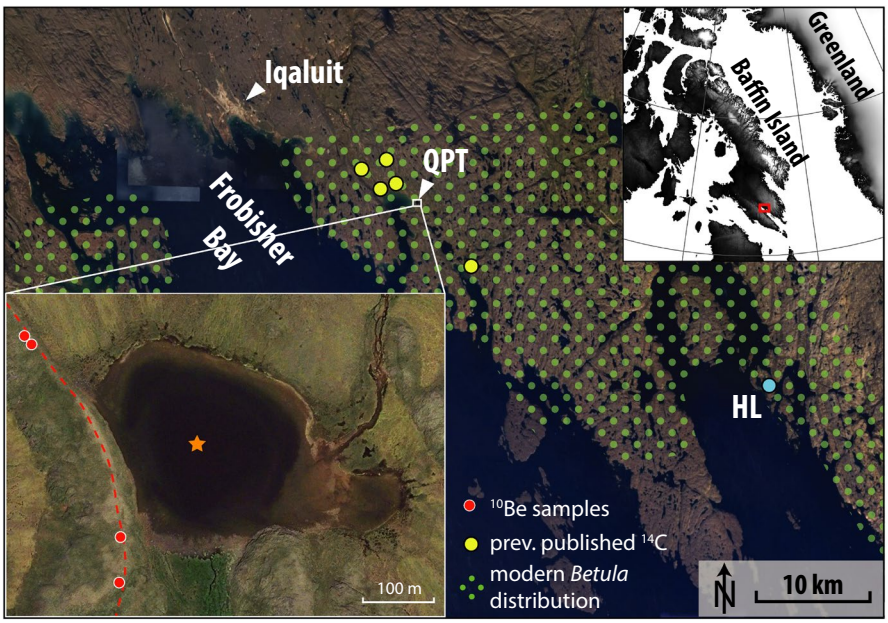

FIGURE 1 Google Earth image of study area on southern Baffin Island, including modern *Betula* distribution from Jacobs, Mode, and Dowdeswell (1985), sites of previously published ^{14}C dates (Andrews & Short, 1983), and site of pollen record mentioned in text (blue circle; HL = Hikwa Lake). Satellite image of Lake Qaupat (QPT; Digital Globe) highlights impounding lateral moraine (dashed red line) with ^{10}Be sample locations and core location (orange star) in the central basin of the lake

2 | MATERIALS AND METHODS

2.1 | Study area

Lake Qaupat (QPT; informal name) is a small (0.08 km^2, max depth 9.2 m) moraine-impounded lake near Frobisher Bay, southern Baffin Island (63.67771°N, 68.19820°W, 35 m a.s.l.; Figure 1). This area was occupied by the Laurentide Ice Sheet during the Last Glacial Maximum and into the early Holocene, until the Foxe Dome sector of the Laurentide Ice Sheet retreated through Frobisher Bay between ~11 and 7 ka (ka = thousands of years before present; Miller, 1980; Squires, 1984). The QPT catchment is 14.5 km^2 with a modern vegetation cover of dwarf-shrub tundra dominated by *Betula glandulosa* (here considered synonymous with *B. nana* spp. *exilis* after Saarela, Sokoloff, & Bull, 2017), *Salix* spp. (willow), other ericaceous shrubs, and sedges. Dwarf birch is near its northern limit at QPT (Figure 1), except for a few isolated populations around southeastern Baffin Island where it grows in favorable microclimates and protected pockets (Andrews, Mode, & Davis, 1980; Andrews, Mode, Webber, Miller, & Jacobs, 1980; Jacobs, Mode, & Dowdeswell, 1985). The present discontinuous distribution of *B. glandulosa* on Baffin Island and Greenland indicates that other factors besides summer temperature—including possibly timing of deglaciation—may help explain its distribution, but it is generally viewed as a climate indicator and a representative species of Low Arctic tundra (Fredskild, 1991; Jacobs, Mode, Squires, & Miller, 1985). Pollen records from this area, including nearby Hikwa Lake (Figure 1; Kerwin, Overpeck, Webb, & Anderson, 2004; Mode & Jacobs, 1987), suggest the continuous postglacial presence of *Betula*, although long-distance wind transport introduced exotic pollen from *Alnus* (alder), *Picea* (spruce), and *Pinus* (pine)—none of which grow on Baffin Island today—into these records, rendering the Holocene establishment timing of *Betula* ambiguous.

2.2 | Field sampling

We collected two ~1.5-m lake sediment cores (QPT16-2A and QPT16-3A) in April 2016 using a modified Nesje coring system (Nesje, 1992) from the lake ice. Both cores were taken from the center of the lake's central deep basin in 8.8 and 9.2 m of water. Cores were kept cold in a snowbank for the duration of the field campaign and then stored at 4°C until processing. For moraine exposure dating, we collected the top 2–4 cm of moraine-crest boulders using a hammer and chisel. We recorded sample locations and elevations with a Garmin Global Positioning System. Topographic shielding at the site is negligible, and we observed that the moraine crest was windswept and snow free in spring 2016, suggesting that snow shielding is negligible as well.

2.3 | ^{10}Be exposure dating

Laboratory processing took place at the University of Colorado Cosmogenic Isotope Laboratory. Rock samples were crushed and sieved to isolate the 250–550 µm fraction, which was then etched in dilute HCl and HF-HNO_3 acids to remove any organics and non-quartz minerals. Further removal of feldspars and mafic minerals was completed via froth flotation followed by heavy liquid separation, and final etching in HF-HNO_3 yielded sufficiently clean quartz as determined by inductively coupled plasma optical emission spectrometry. Chemical procedures for the isolation of beryllium were modified from Kohl & Nishiizumi, 1992; von Blanckenburg, Belshaw, & O'Nions, 1996. We spiked 30 g of quartz with ^{9}Be carrier (Table S1) and then dissolved the samples in HF-HNO_3. Samples were converted to sulfides and then chlorides using H_2SO_4 and HCl, respectively. Fe and Ti were removed through high pH precipitation, followed by precipitation of Be and Al at pH 8. Be was separated from Al and other remaining ions via cation column chromatography. $Be(OH)_2$ was precipitated at pH 8, dried, and combusted to form BeO, and then mixed with Niobium powder and packed into steel cylinders. One process blank was prepared. ^{10}Be/^{9}Be isotope ratio measurements were made via accelerator mass spectrometry (AMS) at the Purdue Rare Isotope Measurement Lab. Ages were calibrated using the CRONUS–Earth online calculator with the Baffin Bay production rate (Young, Schaefer, Briner, & Goehring, 2013) and the time-constant scaling scheme of Lal (1991) and Stone (2000). We evaluated the spread in ages (i.e., determined whether the distribution of ages was primarily caused by measurement uncertainty or 'geologic uncertainty', altered inventories of ^{10}Be due to inheritance or postdepositional disturbance of the boulder) using the reduced chi-squared statistic after Balco (2011). A reduced chi-squared value of ~1 or less indicates that the spread of ages is likely due to measurement uncertainty rather than geologic uncertainty.

2.4 | Core sampling and description

Core QPT16-2A was split and opened in a dedicated ancient DNA clean laboratory at Curtin University in June 2016. We sampled for *sed*aDNA, BSi, and radiocarbon (plant macrofossils) following standard protocols for aDNA sampling (e.g., full clean laboratory personal protective equipment, bleaching, and UV irradiation of sample tools; see Supporting information). Core QPT16-3A was split and opened at the University of Colorado and one-half sampled for brGDGT analyses and radiocarbon. The archive half was transported to the University of Minnesota LacCore facility for split-core multisensor scanning including high-resolution point sensor magnetic susceptibility. The archive half was subsequently analyzed using an ITRAX X-ray fluorescence (XRF) core scanner at the University of Massachusetts, Amherst, to determine elemental abundances. Scans were carried out using a molybdenum tube with a downcore resolution of 300 µm. The voltage and current were set to 30 kV and 55 mA, respectively, with an XRF count time of 10 s.

2.5 | Radiocarbon dating and age model

Previously published radiocarbon ages were recalibrated using CALIB 7.1 (Stuiver, Reimer, & Reimer, 2018) with the Marine13

calibration curve (Reimer et al., 2013) and a reservoir correction (ΔR) of 150 ± 60 years based on the recommended ΔR for southeast Baffin Island (Coulthard, Furze, Pieńkowski, Chantel Nixon, & England, 2010). For lake sediment radiocarbon dating, plant macrofossils were cleaned in deionized water and freeze-dried before undergoing acid-base-acid pretreatment and conversion to graphite at the INSTAAR Laboratory for AMS Radiocarbon Preparation and Research lab. ^{14}C measurements were made at the UC Irvine AMS facility. We calibrated radiocarbon ages and produced age-depth models using a smooth-spline function in the R Software package CLAM version 2.2 (Blaauw, 2010), which relies on the IntCal13 calibration curve (Reimer et al., 2013). The composite core age model includes radiocarbon ages from both cores, with depth correlation based on two sets of statistically overlapping radiocarbon ages (Figure 2; Table S2). Composite depths account for minor differences in upper sediment dewatering.

2.6 | sedaDNA extraction and analysis

Sampling, extraction, and analysis of *sed*aDNA using metabarcoding were conducted at the Trace and Environmental DNA Lab at Curtin University. See Supporting information for a description of extraction, PCR, and sequencing methods. Briefly, we extracted *sed*aDNA from 44 samples taken from the full length of core QPT16-2A (Figure 2) <2 months after core collection. Two replicate 500 mg subsamples, taken from the interior of the core to minimize contamination, were digested in a digest buffer following Grealy et al. (2015). One extraction control was prepared for each batch of 11 samples. Sediment digests were concentrated in Vivaspin centrifugal concentrators, added to a binding buffer following Dabney et al. (2013), and purified via MinElute PCR Purification Kit.

Serial dilutions of the extracts (full concentration, 1/5, 1/10) were amplified using quantitative polymerase chain reaction (qPCR) with two universal plant (plastid) assays: the P6 loop of the plastid trnL (UAA) intron (hereafter shortened to 'trnL P6 loop'; Taberlet et al., 2007) and, for a subset of 26 samples, a short region of the chloroplast gene rbcL (CBOL Plant Working Group et al., 2009; Poinar et al., 1998). Primer sequences are listed in Supporting information. Cycle threshold (C_T) values were typically lowest for the 1/5 and 1/10 dilution (ranging from 22 to 28) indicating the presence of PCR inhibitors in the primary (undiluted) extracts. These qPCR data enabled an optimal level of input DNA into each metabarcoding reaction and a robust evaluation (in the absence of inhibition) of down-core *sed*aDNA preservation (Figure S2). Typically, 1/10 dilutions of the original extract were then PCR amplified (two replicates per sample) with unique (never previously used) multiplex identifiers (MID tags) for each metabarcoding assay using a single-step amplification approach. The efficacy of each MID-tagged PCR was tracked using qPCR to ensure robust and consistent amplifications were achieved.

Amplicons were pooled based on qPCR end-points and blended into a sequencing library. The library was prepared for sequencing by ligating on the Illumina adapter to the MID-tagged products using a PCR-free ligation method following Kozarewa and Turner (2011). The ligated library was size-selected via Pippin Prep and then sequenced using a standard MiSeq flow cell following manufacturer instructions.

Sequencing data was processed using Geneious (https://www.geneious.com) v10.2 following the bioinformatics approach of

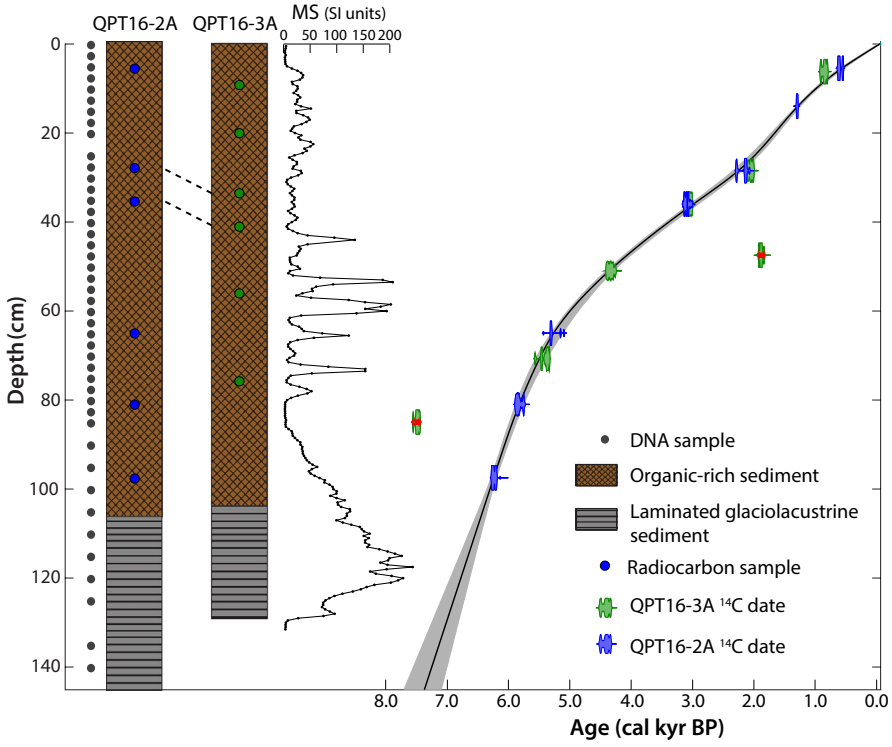

FIGURE 2 Core lithostratigraphy, locations of DNA samples, high-resolution magnetic susceptibility of core QPT16-3A, and composite age–depth model. Blue and green circles indicate locations of plant macrofossils dated with ^{14}C (Table S3), and dashed lines highlight statistically overlapping ages used to correlate the two cores. The age–depth model is plotted on a composite depth scale and was generated with the CLAM smooth-spline function (Blaauw, 2010). Outlier ages are indicated in red; one additional outlier is beyond the scale of this figure (see Table S3)

Coghlan et al. (2015) to identify and remove primers, adapters, and MID tags, filter out short (artifact) sequences and singletons, evaluate read-quality (using Q-scores), and collapse duplicates into unique sequences. Chimeras were identified using USEARCH with the UCHIME de novo method (Edgar, Haas, Clemente, Quince, & Knight, 2011) and removed in Geneious. A Basic Local Alignment Search Tool nucleotide (BLASTn) search was then conducted against the National Centre for Biotechnology Information GenBank database (Altschul, Gish, Pennsylvania, & Park, 1990; Benson et al., 2000). BLAST results were assessed taxonomically in MEtaGenomic ANalyzer v5.10 (Huson, Auch, Qi, & Schuster, 2007; parameters: top 5%, min score 65, min support of 1). Taxonomic results were manually compared with the Arctic plant database of Sønstebø et al. (2010) and the online database Flora of the Canadian Arctic Archipelago (https://nature.ca/aaflora/data). Any taxa not found in the Arctic databases, known food contaminants, and taxa that did not represent >1% of any individual sample were marked as presumed contamination and removed from further analysis. Other than singleton removal, we did not apply an abundance cutoff threshold for accepting a result as a true positive on a per-sample basis because our hypotheses relied more sensitively on avoiding false negatives (i.e., inferring absence relied on a strict requirement of 'zero' reads). Sequencing results from the extraction controls is contained in Table S6 and suggested minimal cross-contamination or laboratory background contamination. rbcL and trnL P6 loop metabarcoding data are available from the Dryad Digital Repository.

In order to assess community-wide changes in vegetation through time, we conducted nonmetric multidimensional scaling (NMDS) ordination analysis (Kruskal, 1964; Paliy & Shankar, 2016; Shi, 1993) on taxonomic abundance data for each primer as well as presence–absence in a combined dataset (collapsed to lowest common taxonomic resolution). We performed NMDS analysis using the R software package vegan (Oksanen et al., 2016; http://CRAN.R-project.org/package=vegan), using the default Bray–Curtis dissimilarity index and 50 iterations for each run. We conducted a permutational analysis of variance (PERMANOVA; Anderson, 2017) to assess the significance of community change through time using the Adonis function within vegan, with a Bray–Curtis dissimilarity matrix and 999 permutations.

2.7 | brGDGT paleothermometry

We estimated past temperatures using the temperature-dependent distribution of bacterial brGDGTs, a class of membrane-spanning lipids produced by bacteria, brGDGTs (Schouten, Hopmans, & Sinninghe Damsté, 2013; Sinninghe, Hopmans, Pancost, Schouten, & Geenevasen, 2000; Weijers, Schouten, van den Donker, Hopmans, & Sinninghe Damsté, 2007). The brGDGT paleothermometer was originally developed for soils but has since been calibrated and applied in lake settings, in which the sedimentary biomarkers are nearly ubiquitous (Pearson et al., 2011; Tierney & Russell, 2009; Zink, Vandergoes, Mangelsdorf, Dieffenbacher-Krall, & Schwark, 2010). Here we rely on an African lake calibration to mean annual air temperature (MAAT), based on the Methylation index of Branched Tetraethers (MBT'_{5Me}) of Russell et al. (2018), as it is currently one of the only lake-based calibration that incorporates the improved chromatographic separation of brGDGT isomers (Hopmans, Schouten, & Sinninghe Damsté, 2016). However, we emphasize that at high-latitude sites, brGDGTs likely reflect summer temperature (Dang et al., 2018; Pearson et al., 2011; Shanahan, Hughen, & Van Mooy, 2013) and that a regional calibration is required for more reliable absolute temperatures. Thus, rather than interpreting absolute temperatures, we focus on prominent changes in mean-normalized temperature anomalies, which are robust across a variety of available calibrations (Figure S5).

Lipids were extracted, filtered, and analyzed for GDGTs via high-performance liquid chromatography–atmospheric pressure chemical ionization–mass spectrometry at the INSTAAR Organic Geochemistry Lab at the University of Colorado Boulder. See Supporting information for full methods.

2.8 | BSi analysis

Samples were ground with a mortar and pestle and mixed with KBr in a 1:50 dilution and analyzed with a Fourier Transform Infrared Spectrometer (FTIRS), following procedures of Liu, Colman, Brown, Minor, and Li (2013) and Vogel, Rosén, Wagner, Melles, and Persson (2008). Measurements were made in triplicate, with the mean and standard deviation presented. While published FTIRS-inferred BSi calibrations indicate a linear relationship between %BSi and absorbance units, the relationship differs between individual lakes (Liu et al., 2013). We thus report BSi in FTIRS absorbance units and only interpret relative changes through the record rather than absolute values.

3 | RESULTS

3.1 | Timing of deglaciation

Four boulder samples from the lateral moraine impounding Lake QPT yielded ^{10}Be exposure ages between 8.2 and 9.8 ka, with a mean and *SD* of 9.1 ± 0.7 ka (Table S1; Figure S1). The reduced chi-squared value for this set of ages is 0.93; thus, the mean age of 9.1 ka is an appropriate estimate of the moraine age. This age is corroborated by calibrated radiocarbon ages on marine shells from ice-proximal deltaic and raised tidal sediments from the Burton Bay region (Figure 1; Andrews & Short, 1983). A mollusk shell in deltaic sediment 6 km SE of QPT (down-paleoflow and thus morphostratigraphically older) dated to 8.9 ± 0.6 cal ka BP (calibrated age in thousands of years before 1950; hereafter shortened to ka), and four sets of marine bivalves from the head of Burton Bay (2–5 km NW of QPT, up-paleoflow) ranged in age from 7.7 to 8.1 ka (Table S2). Together, the ^{10}Be and ^{14}C ages provide compelling evidence that the QPT catchment became ice-free between ~9 and 8 ka, providing a viable substrate for plant colonization after that point.

3.2 | Sediment core description and chronology

We recovered two sediment cores in April 2016, QPT16-2A (1.45 m) and QPT16-3A (1.29 m), taken ~8 m apart in the central basin of Lake QPT (Figure 2). The cores both contained an intact sediment–water interface and ~1 m of gray-brown organic-rich sediment with moss layers underlain by laminated gray-black finer-grained sediment with higher magnetic susceptibility values, likely deposited in a glaciolacustrine setting. Neither of the cores extends into a glacial till, which we presume underlies the glaciolacustrine sediment, indicating that we did not capture the full deglacial sequence. See Supporting information text and Figure S3 for elemental abundance results.

Twelve radiocarbon dates from plant macrofossils, six from each core, went into a composite smooth-spline age-depth model after discarding three outlier ages (Table S3; Figure 2). The outliers were each >25 *SD*s from the mean modeled age, likely due to discrete stratigraphic reworking events. Two sets of statistically overlapping ages were used to correlate the cores, accounting for minor differences in dewatering compaction in their upper portions; see Supporting information text for additional core correlation details. The age model produced extrapolated basal ages of 7.4 ± 0.3 ka (2σ uncertainty) in core QPT16-2A and 6.8 ± 0.2 ka in core QPT16-3A. These basal ages have relatively large uncertainty due to a lack of datable material below 1 m core depth; however, most of the core, and the interval on which we focus our interpretation, has much lower uncertainty, with an average 2σ error of 57 years from 6.5 ka to present. The difference between the moraine age (9.1 ± 0.7 ka) and the basal age of QPT16-2A (7.4 ± 0.3 ka) is primarily due to the lack of recovery of the full deglacial sequence. The age model also revealed a decrease in sedimentation rate after 5.0 ka; higher sedimentation rates prior to 5 ka may be a result of more clastic material on the landscape following deglaciation and/or higher productivity prior to 5 ka.

3.3 | Paleovegetation from sedaDNA

All 44 sediment samples, taken at an average temporal resolution of 170 years (Figure 2) yielded amplifiable plant DNA using the two universal plant assays, trnL P6 loop (all samples) and rbcL (subset of 26 samples). qPCR threshold cycle (C_T) values, indicative of PCR amplification success and thus the quantity of suitable target sequences for amplification, averaged 25.3 for the trnL P6 loop assays and did not systematically decrease downcore, indicating that DNA preservation was sufficiently high for the full 7.4 ka record (Figure S2). Following data deconvolution and initial filtering (see Supporting information), the full trnL P6 loop dataset yielded 637,849 reads (average 14,497 per sample); after final quality filtering, these yields decreased to 633,783 reads (average 14,404 per sample; Tables S4 and S5; Figure S2). The rbcL dataset yielded 174,969 reads (average 6,729 per sample) before final filtering and 170,098 reads (average 6,542 per sample) after final filtering. Following final quality filtering, trnL P6 loop assays yielded 13 distinct taxa with a mean of 8.4 per sample, and rbcL yielded 22 taxa with a mean of 8.4 per sample (Tables S4 and S5; Figure S2). Seven of these taxa were represented by both trnL P6 loop and rbcL, although typically at different taxonomic resolution; for example, the trnL P6 loop assay allowed for the identification of *Empetrum nigrum* (crowberry) to species level, whereas rbcL did not provide a discrimination beyond the Ericaceae family level. Importantly, both metabarcoding assays consistently captured the two dominant deciduous shrubs in this area, *Salix* and *Betula* (Figure 3). Because PCR amplification results in sequence abundance that may not be representative of original copy numbers in a sample, we focused our analysis on presence/absence and normalized data.

Salix was present in both records (to genus level for rbcL and tribe level, Saliceae, for trnL P6 loop) throughout the full core, with absence in only four of 44 samples in one of two plant assays. Conversely, *Betula* (identified to genus level in trnL P6 loop and family level, Betulaceae, in rbcL) was absent for the lowest 50 cm of the core in both assays—10 samples for trnL P6 loop and six samples for rbcL. *Betula*'s initial appearance differed by just one sample interval (~70 years) for the two metabarcoding assays and subsequently remained present throughout the rest of the record (Figure 3). The consistent presence of *Salix* DNA from the base of the core serves as a taphonomic control, indicating that the sudden *Betula* appearance was unlikely to be an artifact of poor preservation below that level. Thus,

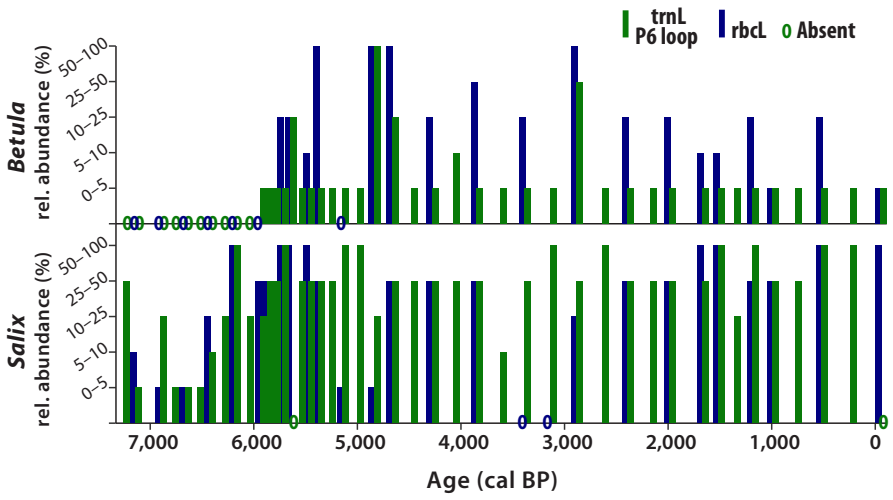

FIGURE 3 *seda*DNA metabarcoding results for two woody shrubs. Downcore record of *Betula* and *Salix*, plotted as relative abundance of taxa (as a percentage of total post-filtered sample reads) for each sample and binned, for trnL P6 loop (green) and rbcL (blue) assays. *Betula* appears in the record at 5.9 ka, whereas *Salix* is present throughout the core

we argue this approach successfully identified the colonization timing of dwarf birch, at 5.9 ± 0.1 ka, as corroborated by two genetic markers.

Nonmetric multidimensional scaling analysis of the trnL P6 loop abundance data yielded a minimum stress of 0.18, indicating that the ordination represented the full dataset reasonably well. The biplot in Figure 4 represents community composition in reduced dimensionality space, defined by NMDS axes 1 and 2, such that samples plotting more closely together had more similar plant communities. A sample age overlay reveals a coherent temporal trend, which is driven primarily by a decrease in NMDS axis 1 values from early to mid-Holocene samples (Figure 4), and a later increase in NMDS axis 2 values. PERMANOVA confirms that plant communities differed significantly between the early (>6 ka; n = 10) and later (<6 ka; n = 34) intervals of the record (pseudo-F = 9.90, p < .001). NMDS taxa scores provide further insight into what drove these community trends through time. Because aquatic taxa (*Callitriche* spp. and *Myriophyllum sibiricum*) plot most strongly on NMDS axis 1, a decrease in axis 1 values from early to mid-Holocene likely signifies a decrease in aquatic plants. Indeed, in the combined metabarcoding dataset, *M. sibiricum* is absent after 4.9 ka and *Callitriche* spp. are absent after 4.3 ka following their dominance early in the record (Tables S4 and S5).

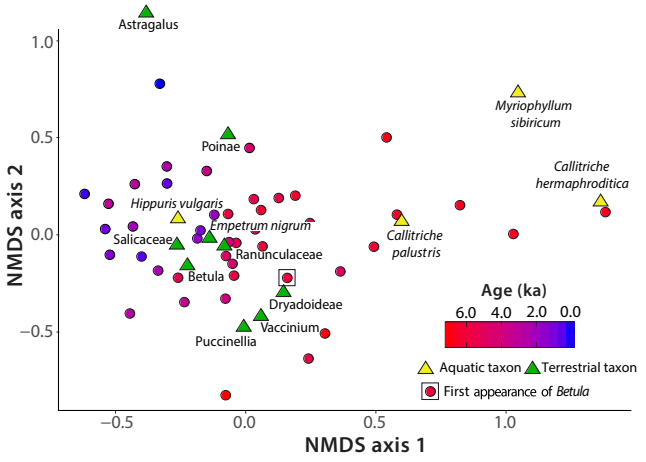

FIGURE 4 Nonmetric multidimensional scaling (NMDS) axes 1 and 2 biplot for trnL P6 loop assays, with sample age overlay and taxa scores

3.4 | Paleoclimate proxies: brGDGT-inferred temperatures and BSi

All 27 samples from core QPT16-3A yielded sufficient concentrations of brGDGTs for temperature estimates using multiple calibrations (Figure S5). Calculated temperatures were highest early in the record, with positive anomalies ranging from 1.4 to 3.7°C and between 6.7 and 6.3 ka (Figure 5) based on a recent lake calibration

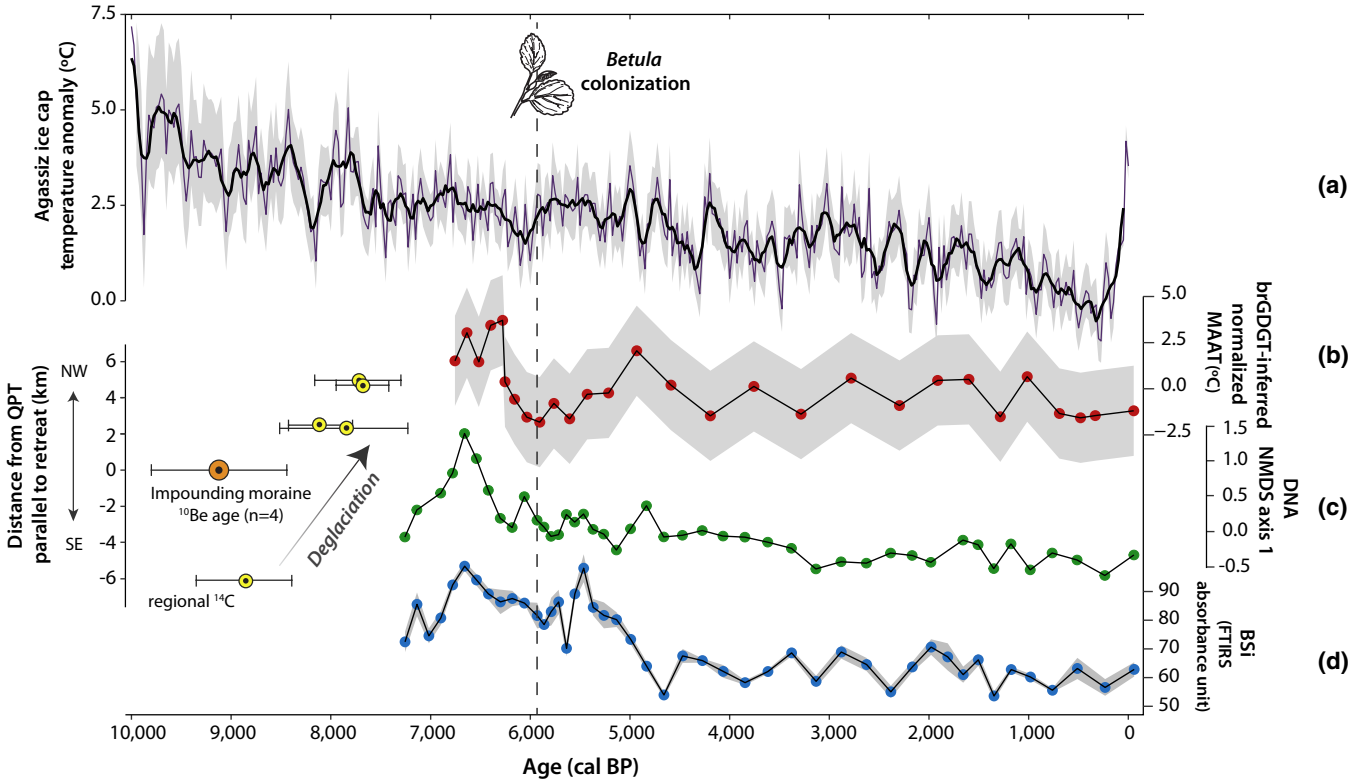

FIGURE 5 Paleoenvironmental reconstruction from Lake Qaupat (QPT). (a) δ^{18}O-inferred temperature reconstruction for the last 10 ka from the Agassiz Ice Cap (Lecavalier et al., 2017). (b) Branched glycerol dialkyl glycerol tetraethers (BrGDGT)-inferred mean annual air temperature (mean-normalized, with calibration root mean squared error as gray band; Russell et al., 2018). (c) Nonmetric multidimensional scaling (NMDS) axis 1 scores from DNA metabarcoding results (trnL P6 loop only). (d) Relative biogenic silica (BSi) concentration (with *SD* as gray band). Dashed line indicates *Betula* colonization at 5.9 ka. Mean ^{10}Be age of the lake-impounding moraine (orange) and regional radiocarbon ages (Andrews & Short, 1983; yellow) constrain progressive deglaciation over the study area

(Russell et al., 2018). At ~6.2 ka, temperatures dropped rapidly, with negative anomalies persisting through 5.2 ka. A transient warming centered at 4.9 ka preceded diminished and less variable temperatures for the remainder of the record. Given the calibration root mean squared error of 2.4°C (Russell et al., 2018), we subsequently focus on the changes that exceeded the uncertainty envelope of the paleothermometer—primarily the shift from warmer to cooler temperatures centered at ~6.2 ka.

We also investigated paleoclimate qualitatively using FTIRS-inferred BSi (Liu et al., 2013; Vogel et al., 2008). BSi concentrations represent diatom abundance and productivity in lakes (Conley, 1988; Conley & Schelske, 2001) and by proxy, spring or summer temperature (Geirsdóttir, Miller, Thordarson, & Ólafsdóttir, 2009; McKay, Kaufman, & Michelutti, 2008), although other factors like nutrient availability can also affect BSi concentration. BSi values were highest early in the record, peaking at 6.6 ka before declining steadily through 5.9 ka (Figure 5). Following a temporary uptick centered at 5.5 ka, BSi values dropped to lower and less variable levels for the remaining 5.0 ka of the record, coinciding with a decrease in sedimentation rate.

4 | DISCUSSION

Taken together, the proxy data outline the postglacial climatic and ecological evolution of the QPT catchment on Baffin Island, Arctic Canada. Following deglaciation after 9.1 ka, the catchment became available for primary terrestrial succession and lake ontogeny. Our *sed*aDNA data indicate that by the start of the lake sediment record at 7.4 ka, soil development and ecological succession had proceeded sufficiently to facilitate the establishment of vascular plants including *Salix*, *Vaccinium* (blueberry genus), and *E. nigrum* (Table S3). A peak in algal productivity, defined by maximum BSi values, is concurrent with a peak in aquatic vegetation, as inferred from NMDS axis 1 values, at 6.7 ka (Figure 5). This relatively productive lake environment was likely a result of high summer lake water temperatures and/or a long ice-free season, and is indeed mirrored in high temperatures inferred from brGDGTs between 6.7 and 6.3 ka. The presence of *Callitriche hermaphroditica* early in the *sed*aDNA record, and its dominance (77%–98% of reads) between 6.8 and 6.4 ka, provides further evidence of warm conditions during this time; in the modern, this species requires minimum July temperatures of ~14°C (Clarke et al., 2018; Väliranta et al., 2015), ~6°C warmer than the modern July mean temperature in Iqaluit. Successional processes and soil development in the surrounding catchment also likely promoted high lacustrine productivity during this time (Engstrom, Fritz, Almendinger, & Juggins, 2000; Fritz & Anderson, 2013). We note that the two QPT sediment cores extend back to only 7.4 and 6.8 ka, respectively, and thus probably miss peak temperatures of the true HTM, which was likely prior to 8 ka in the Eastern Canadian Arctic (Axford, Briner, Miller, & Francis, 2009; Briner et al., 2016; Lecavalier et al., 2017).

All proxy values—brGDGT-inferred temperatures, *sed*aDNA NMDS axis 1, and BSi—then declined in the centuries preceding 6 ka, indicative of a deteriorating climate and waning aquatic productivity. A temporary increase in BSi centered at 5.5 ka signifies that aquatic productivity did not monotonically decline through this period, but the proxies together generally point to warmest conditions and high productivity prior to 6 ka. Additionally, factors other than temperature (e.g., low-oxygen conditions and associated changes in the microbial community) could possibly influence the brGDGT-derived temperature reconstruction (see Supporting information), but our record is consistent with independent proxy data indicating a warmer climate before 6 ka. The pre-6 ka cooling episode was also captured by a peat section from nearby Grinnell Bay (~150 km to the east), which contains a prominent cryoturbated paleosol that dated to 6.3 ± 0.4 ka (Jacobs, Mode, Squires, et al., 1985). Moreover, a δ^{18}O-inferred temperature reconstruction from the Agassiz ice cap also suggests modest cooling from 6.5 to 6.0 ka, and, more broadly, that the warmest temperatures of the Holocene occurred before 6 ka (Figure 5; Lecavalier et al., 2017). Given the multi-proxy evidence for declining temperatures prior to 6 ka, it is surprising to find strong evidence for the colonization of *Betula*—a temperature-sensitive shrub—at 5.9 ka. The catchment was likely ice-free ~3 ka prior, and soil development allowed for the establishment of *Salix* and other tundra plants at least 1.3 ka earlier. Climatic conditions appeared to be warm enough for *Betula* establishment from the start of the record, and subsequently declined markedly. Yet dwarf birch did not become established during peak temperatures, as would be predicted by a rapid dispersal model (Alsos et al., 2007), but instead colonized after several centuries of deteriorating climate. This finding suggests that dispersal mechanisms, whether by bird, sea ice, or other means (Alsos, Ehrich, et al., 2016; Alsos, Sjögren, et al., 2016; Birks, 2008), may have in fact been a limiting factor in shrub colonization of southern Baffin Island. The earlier colonization of *Salix* versus *Betula* could reflect more proximal source areas or taxa-specific dispersal limitations.

The *sed*aDNA results indicating the delayed arrival of *Betula* contradict the interpretation of a palynological record from nearby Hikwa Lake that contains *Betula* pollen throughout its ~8 ka extent (Mode & Jacobs, 1987), a feature that is ubiquitous among pollen records from the region (Gajewski, 2015a; Kerwin et al., 2004). This contrast highlights the different source areas of pollen versus *sed*aDNA. Pollen can be wind-transported long distances, such that tree species from within the *Betula* genus, which produce large amounts of pollen that is difficult to distinguish from that of *Betula* shrub species, are likely contributing exotic pollen from northeastern mainland Canada (Kerwin et al., 2004). This issue is particularly problematic in treeless landscapes where local pollen production is relatively low and wind transport of some pollen types is highly effective (Birks, 2008). Alternatively, the fact that the *sed*aDNA indicated no *Betula* from early in the record even when exotic *Betula* pollen was likely present supports other recent work concluding that *sed*aDNA has a predominantly local source from within a lake catchment (Alsos et al., 2018; Niemeyer, Epp, Stoof-Leichsenring,

Pestryakova, & Herzschuh, 2017; Sjögren et al., 2016) and is not derived from pollen grains (at least with standard extraction techniques; see Parducci et al., 2017). The DNA-based colonization timing of *Betula* at 5.9 ka coincides with an increase in *Betula* pollen in the Hikwa lake record at ~6 ka (Mode & Jacobs, 1987), which we suggest results from a shift from background-exotic flux to additional locally sourced *Betula* pollen.

Our combination of molecular proxies reveals that a temperature-sensitive shrub became established significantly after optimal climatic conditions and remained present through the cooler conditions of the late Holocene. Taken more broadly, this supports the notion that some types of thermophilous vegetation may lag climate on the order of 1,000 years (Davis & Shaw, 2001; Prentice, Bartlein, & Webb, 1991)—particularly in the Arctic, where migration distances can be vast and rapid climate changes are pronounced. The presence of a migration barrier (Hudson Strait) from the presumed southern source area in this case also likely decreased the efficiency of dispersal (Davis, Woods, Webb, & Futyma, 1986). Similar lags in shrub migration have been noted in Greenland, with *Betula* arriving between 8 and 6 ka and *Alnus* later yet, at ~4 ka (Bennike, 1999; Fredskild, 1991; Gajewski, 2015a). In contrast, studies from other remote Arctic islands, including Svalbard and Iceland, have suggested rapid postglacial shrub colonization (Alsos, Ehrich, et al., 2016; Alsos, Sjögren, et al., 2016; Rundgren & Ingólfsson, 1999). This is the first definitive evidence from the Canadian Arctic Archipelago of a shrub migration lag, possibly because of the proximity of tree pollen sources.

One consequence of a sluggish vegetation response to climate is that pollen-based temperature reconstructions may inaccurately capture the timing of past climate change. Indeed, a temperature reconstruction based on the Hikwa Lake pollen record yields peak Holocene summer temperatures between 4.2 and 3.2 ^{14}C years BP (4.7–3.4 ka) when *Betula* pollen is at its maximum (Kerwin et al., 2004). This mid-Holocene rise in *Betula* (as well as *Alnus*) pollen is a common feature of lake records from southern Baffin Island (Briner et al., 2016) and may have been caused by migration lags or greater or more common southerly winds transporting exotic pollen (Kerwin et al., 2004). As a result, palynological records generally point to a later HTM in this region than do ice core records (Lecavalier et al., 2017) or chironomid-inferred temperature reconstructions (Axford et al., 2009) and may introduce a time-lag bias for Arctic proxy compilations (Gajewski, 2015b; Kaufman et al., 2004).

Dispersal-limited migration for certain woody plant species may limit the rate of current and future Arctic shrubification and delay the impacts of its associated climate feedbacks, particularly for islands or otherwise isolated areas. Importantly, however, migration is a necessary mechanism for vegetation to respond to rapid climate change (Aitken, Yeaman, Holliday, Wang, & Curtis-McLane, 2008; Chen, Hill, Ohlemüller, Roy, & Thomas, 2011; Thuiller et al., 2008). If migration barriers can result in delays on the order of 1,000 years, as seems to have been the case in the postglacial past on Baffin Island, species may not be able to shift their ranges quickly enough to keep up with rapidly shifting environmental conditions where geographic barriers exist. We note that dispersal limitations are species-specific (Thuiller et al., 2008) and barrier-specific, and additional paleoecological work is required to broaden our understanding of high-latitude vegetation dynamics. Insights from such paleovegetation reconstructions can be used to improve the representation of vegetation-related feedbacks in earth system models and validate species distribution models (Guisan & Wilfried, 2005), both of which are critical in predicting the climatic and ecological future of the planet.

ACKNOWLEDGEMENTS

The authors thank the Inuit and government of Nunavut for access to the field site (Nunavut Research Institute license # 01 019 16N-A). We are grateful for field assistance from T. Lee and logistical assistance from R. Armstrong, K. Smith, and Nunavut Arctic College. We thank G.A. de Wet, A. Todd, L. Springett, A. Samples, C.R. Florian, D.J. Harning, S.L. Pendleton, A. Grealy, D. Murray, and D. Werndly for laboratory assistance, J.H. Raberg for thoughtful discussion, and M.K. Raynolds for modern vegetation insights. We acknowledge the INSTAAR Radiocarbon Prep Lab, UC Irvine AMS Facility, and the Purdue Rare Isotope Measurement Lab for providing isotope measurements, the Pawsey supercomputing facility at Curtin University for bioinformatic services, the University of Minnesota LacCore Facility for core scanning, and the University of Massachusetts Amherst ITRAX facility for μXRF data. Contributions of S.E.C. were supported by an NSF Graduate Research Fellowship under grant DGE1144083 and the GRFP GROW program. Research funding was provided by NSF awards BCS1657743 (S.E.C.) and ARC1737712 (G.H.M., J.S., M.B.), a National Geographic Society Early Career Grant, a Geological Society of America student grant, the CU Department of Geological Sciences, the CU Center for the Study of Origins, and INSTAAR. The manuscript benefited from insightful feedback from three anonymous reviewers.

CONFLICT OF INTEREST

The authors report no conflict of interest.

ORCID

Sarah E. Crump https://orcid.org/0000-0002-6606-7350
Julio Sepúlveda https://orcid.org/0000-0002-8251-6937
Michael Bunce https://orcid.org/0000-0002-0302-4206

REFERENCES

Aitken, S. N., Yeaman, S., Holliday, J. A., Wang, T., & Curtis-McLane, S. (2008). Adaptation, migration or extirpation: Climate change outcomes for tree populations. *Evolutionary Applications*, *1*, 95–111. https://doi.org/10.1111/j.1752-4571.2007.00013.x

Alsos, I. G., Ehrich, D., Seidenkrantz, M. S., Bennike, O., Kirchhefer, A. J., & Geirsdottir, A. (2016). The role of sea ice for vascular plant dispersal in the Arctic. *Biology Letters*, *12*(9), 2016–2019. https://doi.org/10.1098/rsbl.2016.0264

Alsos, I. G., Eidesen, P. B., Ehrich, D., Skrede, I., Westergaard, K., Jacobsen, G. H., … Brochmann, C. (2007). Frequent long-distance plant colonization in the changing Arctic. *Science*, *316*(5831), 1606–1609. https://doi.org/10.1126/science.1139178

Alsos, I. G., Lammers, Y., Yoccoz, N. G., Jørgensen, T., Sjögren, P., Gielly, L., & Edwards, M. E. (2018). Plant DNA metabarcoding of lake sediments: How does it represent the contemporary vegetation. *PLoS ONE*, *13*(4), e0195403. https://doi.org/10.1371/journal.pone.0195403

Alsos, I. G., Sjögren, P., Edwards, M. E., Landvik, J. Y., Gielly, L., Forwick, M., Pedersen, M. W. (2016). Sedimentary ancient DNA from Lake Skartjorna, Svalbard: Assessing the resilience of arctic flora to Holocene climate change. *The Holocene*, *26*, 627–642. https://doi.org/10.1177/0959683615612563

Altschul, S. F., Gish, W., Miller, W., Myers, E. W., & Lipman, D. J. (1990). Basic local alignment search tool. *Journal of Molecular Biology*, *215*, 403–410. https://doi.org/10.1016/S0022-2836(05)80360-2

Anderson, M. J. (2017). Permutational multivariate analysis of variance (PERMANOVA). *Wiley StatsRef: Statistics Reference Online*, 1–15. https://doi.org/10.1002/9781118445112.stat07841

Anderson-Carpenter, L. L., McLachlan, J. S., Jackson, S. T., Kuch, M., Lumibao, C. Y., & Poinar, H. N. (2011). Ancient DNA from lake sediments: Bridging the gap between paleoecology and genetics. *BMC Evolutionary Biology*, *11*(1), 30. https://doi.org/10.1186/1471-2148-11-30

Andrews, A. J. T., Mode, W. N., & Davis, P. T. (1980). Holocene climate based on pollen transfer functions, Eastern Canadian Arctic. *Arctic and Alpine Research*, *12*(1), 41–64. https://doi.org/10.2307/1550589

Andrews, J. T., Mode, W. N., Webber, P. J., Miller, G. H., & Jacobs, J. D. (1980). Report on the distribution of dwarf birches and present pollen rain, Baffin Island, N.W.T., Canada. *Arctic*, *33*(1), 50–58. https://doi.org/10.14430/arctic2547

Andrews, J., & Short, S. (1983). Radiocarbon date list V: Baffin Island, N.W.T., University of Colorado, Institute of Arctic and Alpine Research, Occasional Paper No. 40. ISSN 0069-614.

Axford, Y., Briner, J. P., Miller, G. H., & Francis, D. R. (2009). Paleoecological evidence for abrupt cold reversals during peak Holocene warmth on Baffin Island, Arctic Canada. *Quaternary Research*, *71*(2), 142–149. https://doi.org/10.1016/j.yqres.2008.09.006

Balco, G. (2011). Contributions and unrealized potential contributions of cosmogenic-nuclide exposure dating to glacier chronology, 1990–2010. *Quaternary Science Reviews*, *30*(1–2), 3–27. https://doi.org/10.1016/j.quascirev.2010.11.003

Bennike, O. (1999). Colonisation of Greenland by plants and animals after the last ice age: A review. *Polar Record*, *35*(195), 323–336. https://doi.org/10.1017/S0032247400015679

Benson, D. A., Cavanaugh, M., Clark, K., Karsch-Mizrachi, I., Lipman, D. J., Ostell, J., & Sayers, E. W. (2000). GenBank. *Nucleic Acids Research*, *28*, 15–18. https://doi.org/10.1093/nar/gks1195

Birks, H. H. (2008). The Late-Quaternary history of arctic and alpine plants. *Plant Ecology & Diversity*, *1*(2), 135–146. https://doi.org/10.1080/17550870802328652

Birks, H. H., & Birks, H. J. B. (2000). Future uses of pollen analysis must include plant macrofossils. *Journal of Biogeography*, *27*(1), 31–35. https://doi.org/10.1046/j.1365-2699.2000.00375.x

Blaauw, M. (2010). Methods and code for 'classical' age-modelling of radiocarbon sequences. *Quaternary Geochronology*, *5*, 512–518. https://doi.org/10.1016/j.quageo.2010.01.002

Bonfils, C. J. W., Phillips, T. J., Lawrence, D. M., Cameron-Smith, P., Riley, W. J., & Subin, Z. M. (2012). On the influence of shrub height and expansion on northern high latitude climate. *Environmental Research Letters*, *7*(1), 015503. https://doi.org/10.1088/1748-9326/7/1/015503

Briner, J. P., McKay, N. P., Axford, Y., Bennike, O., Bradley, R. S., de Vernal, A., … Wagner, B. (2016). Holocene climate change in Arctic Canada and Greenland. *Quaternary Science Reviews*, *147*, 340–364. https://doi.org/10.1016/j.quascirev.2016.02.010

CBOL Plant Working Group; Hollingsworth, P. M., Forrest, L. L., Spouge, J. L., Hajibabaei, M., Ratnasingham, S., van der Bank, M., …Little, D. P. (2009). A DNA barcode for land plants. *Proceedings of the National Academy of Sciences of the United States of America*, *106*(31), 12794–12797. https://doi.org/10.1073/pnas.0905845106

Chapin, F. S., Shaver, G. R., Giblin, A. E., Nadelhoffer, K. J., & Laundre, J. A. (1995). Responses of Arctic Tundra to experimental and observed changes in climate. *Ecology*, *76*(3), 694–711. https://doi.org/10.2307/1939337

Chen, I., Hill, J. K., Ohlemüller, R., Roy, D. B., & Thomas, C. D. (2011). Rapid range shifts of species associated with high levels of climate warming. *Science*, *333*, 1024–1027. https://doi.org/10.1126/science.1206432

Clarke, C. L., Edwards, M. E., Brown, A. G., Gielly, L., Lammers, Y., Heintzman, P. D., … Alsos, I. G. (2018). Holocene floristic diversity and richness in northeast Norway revealed by sedimentary ancient DNA (sedaDNA) and pollen. *Boreas*, *48*, 299–316. https://doi.org/10.1111/bor.12357

Coghlan, M. L., Maker, G., Crighton, E., Haile, J., Murray, D. C., White, N. E., … Bunce, M. (2015). Combined DNA, toxicological and heavy metal analyses provides an auditing toolkit to improve pharmacovigilance of traditional Chinese medicine (TCM). *Scientific Reports*, *5*(December), 1–9. https://doi.org/10.1038/srep17475

Conley, D. J. (1988). Biogenic silica as an estimate of siliceous microfossil abundance in Great Lakes sediments. *Biogeochemistry*, *6*(3), 161–179. https://doi.org/10.1007/BF02182994

Conley, D. J., & Schelske, C. L. (2001). Biogenic silica. In J. Smol, H. Birks, & W. Last (Eds.), *Tracking environmental change using lake sediments. Terrestrial, algal, and siliceous indicators* (Vol. *3*, pp. 1–13). Dordrecht, the Netherlands: Kluwer Academic Publishers.

Coulthard, R. D., Furze, M. F. A., Pieńkowski, A. J., Chantel Nixon, F., & England, J. H. (2010). New marine ΔR values for Arctic Canada. *Quaternary Geochronology*, *5*(4), 419–434. https://doi.org/10.1016/j.quageo.2010.03.002

Dabney, J., Knapp, M., Glocke, I., Gansauge, M.-T., Weihmann, A., Nickel, B., … Meyer, M. (2013). Complete mitochondrial genome sequence of a Middle Pleistocene cave bear reconstructed from ultrashort DNA fragments. *Proceedings of the National Academy of Sciences of the United States of America*, *110*(39), 15758–15763. https://doi.org/10.1073/pnas.1314445110

Dang, X., Ding, W., Yang, H., Pancost, R. D., Naafs, B. D. A., Xue, J., … Xie, S. (2018). Different temperature dependence of the bacterial brGDGT isomers in 35 Chinese lake sediments compared to that in soils. *Organic Geochemistry*, *119*, 72–79. https://doi.org/10.1016/j.orggeochem.2018.02.008

Davis, M. B., & Shaw, R. G. (2001). Range shifts and adaptive responses to quaternary climate change. *Science*, *292*(April), 673–680. https://doi.org/10.1126/science.292.5517.673

Davis, M., Woods, K., Webb, S., & Futyma, R. (1986). Dispersal versus climate: Expansion of *Fagus* and *Tsuga* into the Upper Great Lakes region. *Vegetatio*, *67*, 93–103. https://doi.org/10.1007/BF00037360

Edgar, R. C., Haas, B. J., Clemente, J. C., Quince, C., & Knight, R. (2011). UCHIME improves sensitivity and speed of chimera detection. *Bioinformatics*, *27*(16), 2194–2200. https://doi.org/10.1093/bioinformatics/btr381

Elmendorf, S. C., Henry, G. H. R., Hollister, R. D., Björk, R. G., Boulanger-Lapointe, N., Cooper, E. J., … Wipf, S. (2012). Plot-scale evidence of tundra vegetation change and links to recent summer warming. *Nature Climate Change*, *2*(June), 8–12. https://doi.org/10.1038/nclimate1465

Engstrom, D. R., Fritz, S. C., Almendinger, J. E., & Juggins, S. (2000). Chemical and biological trends during lake evolution in

recently deglaciated terrain. *Nature*, *408*(6809), 161–166. https://doi.org/10.1038/35041500

Fauchald, P., Park, T., Tømmervik, H., Myneni, R., & Hausner, V. H. (2017). Arctic greening from warming promotes declines in caribou populations. *Science Advances*, *3*(4), e1601365. https://doi.org/10.1126/sciadv.1601365

Fredskild, B. (1991). The genus *Betula* in Greenland – Holocene history, present distribution and synecology. *Nordic Journal of Botany*, *11*(4), 393–412. https://doi.org/10.1111/j.1756-1051.1991.tb01236.x

Fritz, S. C., & Anderson, N. J. (2013). The relative influences of climate and catchment processes on Holocene lake development in glaciated regions. *Journal of Paleolimnology*, *49*(3), 349–362. https://doi.org/10.1007/s10933-013-9684-z

Gajewski, K. (2015a). Impact of Holocene climate variability on Arctic vegetation. *Global and Planetary Change*, *133*, 272–287. https://doi.org/10.1016/j.gloplacha.2015.09.006

Gajewski, K. (2015b). Quantitative reconstruction of Holocene temperatures across the Canadian Arctic and Greenland. *Global and Planetary Change*, *128*, 14–23. https://doi.org/10.1016/j.gloplacha.2015.02.003

Geirsdóttir, Á., Miller, G. H., Thordarson, T., & Ólafsdóttir, K. B. (2009). A 2000 year record of climate variations reconstructed from Haukadalsvatn, West Iceland. *Journal of Paleolimnology*, *41*(1), 95–115. https://doi.org/10.1007/s10933-008-9253-z

Goetz, S. J., Bunn, A. G., Fiske, G. J., & Houghton, R. A. (2005). Satellite-observed photosynthetic trends across boreal North America associated with climate and fire disturbance. *Proceedings of the National Academy of Sciences of the United States of America*, *102*(38), 13521–13525. https://doi.org/10.1073/pnas.0506179102

Grealy, A. C., McDowell, M. C., Scofield, P., Murray, D. C., Fusco, D. A., Haile, J., … Bunce, M. (2015). A critical evaluation of how ancient DNA bulk bone metabarcoding complements traditional morphological analysis of fossil assemblages. *Quaternary Science Reviews*, *128*, 37–47. https://doi.org/10.1016/j.quascirev.2015.09.014

Guisan, A., & Wilfried, T. (2005). Predicting species distribution: Offering more than simple habitat models. *Ecology Letters*, *8*, 993–1009. https://doi.org/10.1111/j.1461-0248.2005.00792.x

Hopmans, E. C., Schouten, S., & Sinninghe Damsté, J. S. (2016). The effect of improved chromatography on GDGT-based palaeoproxies. *Organic Geochemistry*, *93*, 1–6. https://doi.org/10.1016/j.orggeochem.2015.12.006

Huson, D., Auch, A., Qi, J., & Schuster, S. (2007). MEGAN analysis of metagenome data. *Gennome Research*, *17*, 377–386. https://doi.org/10.1101/gr.5969107

Jacobs, J. D., Mode, W. N., & Dowdeswell, E. K. (1985). Contemporary pollen deposition and the distribution of *Betula glandulosa* at the limit of Low Arctic tundra in southern Baffin Island, N.W.T., Canada. *Arctic and Alpine Research*, *17*(3), 279–287. https://doi.org/10.2307/1551018

Jacobs, J. D., Mode, W. N., Squires, C. A., & Miller, G. H. (1985). Holocene environmental change in the Frobisher Bay area, Baffin Island, N.W.T.: Deglaciation, emergence, and the sequence of vegetation and climate. *Géographie Physique Et Quaternaire*, *39*(2), 151–162. https://doi.org/10.7202/032599ar

Jacobson, G. J., & Bradshaw, R. (1981). The selection of sites for paleovegetational studies. *Quaternary Research*, *96*(1981), 80–96. https://doi.org/10.1016/0033-5894(81)90129-0

Ju, J., & Masek, J. G. (2016). The vegetation greenness trend in Canada and US Alaska from 1984–2012 Landsat data. *Remote Sensing of Environment*, *176*, 1–16. https://doi.org/10.1016/j.rse.2016.01.001

Kaufman, D. S., Ager, T. A., Anderson, N. J., Anderson, P. M., Andrews, J. T., Bartlein, P. J., … Wolfe, B. B. (2004). Holocene thermal maximum in the western Arctic (0–180°W). *Quaternary Science Reviews*, *23*, 529–560. https://doi.org/10.1016/j.quascirev.2003.09.007

Kerwin, M. W., Overpeck, J. T., Webb, R. S., & Anderson, K. H. (2004). Pollen-based summer temperature reconstructions for the eastern Canadian boreal forest, subarctic, and Arctic. *Quaternary Science Reviews*, *23*, 1901–1924. https://doi.org/10.1016/j.quascirev.2004.03.013

Kohl, C. P., & Nishiizumi, K. (1992). Chemical isolation of quartz for measurement of in-situ-produced cosmogenic nuclides. *Geochimica et Cosmochimica Acta*, *56*, 3583–3587. https://doi.org/10.1016/0016-7037(92)90401-4

Kozarewa, I., & Turner, D. (2011). Amplification-free library preparation for paired-end illumina sequencing. In Y. M. Won & S. C. Ricke (Eds.), *High-throughput next generation sequencing: Methods and applications* (pp. 257–266). Berlin, Germany: Springer Science+Business Media.

Kruskal, J. B. (1964). Nonmetric multidimensional scaling: A numerical method. *Psychometrika*, *29*(2), 115–129. https://doi.org/10.1007/BF02289694

Lal, D. (1991). Cosmic ray labeling of erosion surfaces: In situ nuclide production rates and erosion models. *Earth and Planetary Science Letters*, *104*, 424–439. https://doi.org/10.1016/0012-821X(91)90220-C

Lecavalier, B. S., Fisher, D. A., Milne, G. A., Vinther, B. M., Tarasov, L., Huybrechts, P., … Dyke, A. S. (2017). High Arctic Holocene temperature record from the Agassiz ice cap and Greenland ice sheet evolution. *Proceedings of the National Academy of Sciences of the United States of America*, *114*(23), 5952–5957. https://doi.org/10.1073/pnas.1616287114

Liu, X., Colman, S. M., Brown, E. T., Minor, E. C., & Li, H. (2013). Estimation of carbonate, total organic carbon, and biogenic silica content by FTIR and XRF techniques in lacustrine sediments. *Journal of Paleolimnology*, *50*, 387–398. https://doi.org/10.1007/s10933-013-9733-7

McKay, N. P., Kaufman, D. S., & Michelutti, N. (2008). Biogenic silica concentration as a high-resolution, quantitative temperature proxy at Hallet Lake, south-central Alaska. *Geophysical Research Letters*, *35*(5), 4–9. https://doi.org/10.1029/2007GL032876

Miller, G. H. (1980). Late Foxe glaciation of southern Baffin Island, N.W.T., Canada. *Geological Society of America Bulletin*, *91*(7), 399. https://doi.org/10.1130/0016-7606(1980)91<399:LFGOSB>2.0.CO;2

Mode, W. N., & Jacobs, J. D. (1987). Surficial geology and palynology, Inner Frobisher Bay. In *Glacial geology and Holocene events, southern Baffin Island, N.W.T.: Guidebook for Field Trip C2, 12th International Congress, International Union for Quaternary Research*, Ottawa, ON, pp. 53–62.

Myers-Smith, I. H., Forbes, B. C., Wilmking, M., Hallinger, M., Lantz, T., Blok, D., … Hik, D. S. (2011). Shrub expansion in tundra ecosystems: Dynamics, impacts and research priorities. *Environmental Research Letters*, *6*, 1–15. https://doi.org/10.1088/1748-9326/6/4/045509

Myneni, R. B., Keeling, C. D., Tucker, C. J., Asrar, G., & Nemani, R. R. (1997). Increased plant growth in the northern high latitudes from 1981 to 1991. *Nature*, *386*, 698–702. https://doi.org/10.1038/386698a0

Nesje, A. (1992). A piston corer for lacustrine and marine sediments. *Arctic and Alpine Research*, *24*(3), 257–259. https://doi.org/10.2307/1551667

Niemeyer, B., Epp, L. S., Stoof-leichsenring, K., & Herzschuh, U. (2016). Modern and ancient DNA in lacustrine sediments – Vegetation signals unraveled. In *11th International Conference on Permafrost (ICOP)*. Retrieved from http://epic.awi.de/41409/

Niemeyer, B., Epp, L. S., Stoof-Leichsenring, K. R., Pestryakova, L. A., & Herzschuh, U. (2017). A comparison of sedimentary DNA and pollen from lake sediments in recording vegetation composition at the Siberian treeline. *Molecular Ecology Resources*, *17*(6), e46–e62. https://doi.org/10.1111/1755-0998.12689

Oksanen, J., Blanchet, F. G., Kindt, R., Legendre, P., Minchin, P. R., O'Hara, R., … Wagner, H. (2016). *vegan: Community ecology package*. Retrieved from http://cran.r-project.org/package=vegan

Paliy, O., & Shankar, V. (2016). Application of multivariate statistical techniques in microbial ecology. *Molecular Ecology*, *25*, 1032–1057. https://doi.org/10.1111/mec.13536

Parducci, L., Bennett, K. D., Ficetola, G. F., Alsos, I. G., Suyama, Y., Wood, J. R., & Pedersen, M. W. (2017). Ancient plant DNA in lake sediments. *New Phytologist*, *214*, 924–942. https://doi.org/10.1111/nph.14470

Pearson, E. J., Juggins, S., Talbot, H. M., Weckström, J., Rosén, P., Ryves, D. B., … Schmidt, R. (2011). A lacustrine GDGT-temperature calibration from the Scandinavian Arctic to Antarctic: Renewed potential for the application of GDGT-paleothermometry in lakes. *Geochimica et Cosmochimica Acta*, *75*(20), 6225–6238. https://doi.org/10.1016/j.gca.2011.07.042

Pearson, R. G., Phillips, S. J., Loranty, M. M., Beck, P. S. A., Damoulas, T., Knight, S. J., & Goetz, S. J. (2013). Shifts in Arctic vegetation and associated feedbacks under climate change. *Nature Climate Change*, *3*(7), 673–677. https://doi.org/10.1038/nclimate1858

Poinar, H. N., Hofreiter, M., Spaulding, W. G., Martin, P. S., Stankiewicz, B. A., Bland, H., … Pääbo, S. (1998). Molecular coproscopy: Dung and diet of the extinct ground sloth *Nothrotheriops shastensis*. *Science*, *281*(5375), 402–406. https://doi.org/10.1126/science.281.5375.402

Prentice, I. C., Bartlein, P. J., & Webb, T. I. (1991). Vegetation and climate change in eastern North America since the last glacial maximum. *Ecology*, *72*(6), 2038–2056. https://doi.org/10.2307/1941558

Reimer, P. J., Bard, E., Bayliss, A., Beck, J. W., Blackwell, P. G., Ramsey, C. B., … van der Plicht, J. (2013). IntCal13 and Marine13 radiocarbon age calibration curves 0–50,000 years cal BP. *Radiocarbon*, *46*(4), 1869–1887. https://doi.org/10.2458/azu_js_rc.46.4183

Rundgren, M., & Ingólfsson, Ó. (1999). Plant survival in Iceland during periods of glaciation? *Journal of Biogeography*, *26*(2), 387–396. https://doi.org/10.1046/j.1365-2699.1999.00296.x

Russell, J. M., Hopmans, E. C., Loomis, S. E., Liang, J., & Sinninghe, J. S. (2018). Organic Geochemistry Distributions of 5- and 6-methyl branched glycerol dialkyl glycerol tetraethers (brGDGTs) in East African lake sediment: Effects of temperature, pH, and new lacustrine paleotemperature calibrations. *Organic Geochemistry*, *117*, 56–69. https://doi.org/10.1016/j.orggeochem.2017.12.003

Saarela, J. M., Sokoloff, P. C., & Bull, R. D. (2017). Vascular plant biodiversity of the lower Coppermine River valley and vicinity (Nunavut, Canada): An annotated checklist of an Arctic flora. *PeerJ*, *5*, e2835. https://doi.org/10.7717/peerj.2835

Schouten, S., Hopmans, E. C., & Sinninghe Damsté, J. S. (2013). The organic geochemistry of glycerol dialkyl glycerol tetraether lipids: A review. *Organic Geochemistry*, *54*, 19–61. https://doi.org/10.1016/j.orggeochem.2012.09.006

Shanahan, T. M., Hughen, K. A., & Van Mooy, B. A. S. (2013). Temperature sensitivity of branched and isoprenoid GDGTs in Arctic lakes. *Organic Geochemistry*, *64*, 119–128. https://doi.org/10.1016/j.orggeochem.2013.09.010

Shi, G. R. (1993). Multivariate data analysis in palaeoecology and palaeobiogeography – A review. *Palaeogeography, Palaeoclimatology, Palaeoecology*, *105*(3–4), 199–234. https://doi.org/10.1016/0031-0182(93)90084-V

Sinninghe, J. S., Hopmans, E. C., Pancost, R. D., Schouten, S., & Geenevasen, J. A. J. (2000). Newly discovered non-isoprenoid glycerol dialkyl glycerol tetraether lipids in sediments. *Chemical Communications*, *17*, 1683–1684. https://doi.org/10.1039/b004517i

Sjögren, P., Edwards, M. E., Gielly, L., Langdon, C. T., Croudace, I. W., Merkel, M. K. F., … Alsos, I. G. (2016). Lake sedimentary DNA accurately records 20th Century introductions of exotic conifers in Scotland. *New Phytologist*, *213*, 929–941, https://doi.org/10.1111/nph.14199

Sønstebø, J. H., Gielly, L., Brysting, A. K., Elven, R., Edwards, M., Haile, J., … Brochmann, C. (2010). Using next-generation sequencing for molecular reconstruction of past Arctic vegetation and climate. *Molecular Ecology Resources*, *10*(6), 1009–1018. https://doi.org/10.1111/j.1755-0998.2010.02855.x

Squires, C. A. (1984). The late Foxe deglaciation of the Burton Bay area, southeastern Baffin Island, N.W.T. Electronic Theses and Dissertations. Paper 4084.

Stone, J. O. (2000). Air pressure and cosmogenic isotope production. *Journal of Geophyscial Research*, *105*(B10), 23753–23759. https://doi.org/10.1029/2000JB900181

Stuiver, M., Reimer, P., & Reimer, R. (2018). *CALIB 7.1 [WWW program]*. Retrieved from http://calib.org

Sturm, M., Douglas, T., Racine, C., & Liston, G. E. (2005). Changing snow and shrub conditions affect albedo with global implications. *Journal of Geophysical Research*, *110*(G1), 1–13. https://doi.org/10.1029/2005JG000013

Swann, A. L., Fung, I. Y., Levis, S., Bonan, G. B., & Doney, S. C. (2010). Changes in Arctic vegetation amplify high-latitude warming through the greenhouse effect. *Proceedings of the National Academy of Sciences of the United States of America*, *107*(4), 1295–1300. https://doi.org/10.1073/pnas.0913846107

Taberlet, P., Coissac, E., Pompanon, F., Gielly, L., Miquel, C., Valentini, A., … Willerslev, E. (2007). Power and limitations of the chloroplast trnL (UAA) intron for plant DNA barcoding. *Nucleic Acids Research*, *35*(3), e14–e14. https://doi.org/10.1093/nar/gkl938

Tape, K., Sturm, M., & Racine, C. (2006). The evidence for shrub expansion in Northern Alaska and the Pan-Arctic. *Global Change Biology*, *12*(4), 686–702. https://doi.org/10.1111/j.1365-2486.2006.01128.x

Thuiller, W., Albert, C., Araújo, M. B., Berry, P. M., Cabeza, M., Guisan, A., … Zimmermann, N. E. (2008). Predicting global change impacts on plant species' distributions: Future challenges. *Perspectives in Plant Ecology, Evolution and Systematics*, *9*, 137–152. https://doi.org/10.1016/j.ppees.2007.09.004

Tierney, J. E., & Russell, J. M. (2009). Distributions of branched GDGTs in a tropical lake system: Implications for lacustrine application of the MBT/CBT paleoproxy. *Organic Geochemistry*, *40*(9), 1032–1036. https://doi.org/10.1016/j.orggeochem.2009.04.014

Väliranta, M., Salonen, J. S., Heikkilä, M., Amon, L., Helmens, K., Klimaschewski, A., … Birks, H. H. (2015). Plant macrofossil evidence for an early onset of the Holocene summer thermal maximum in northernmost Europe. *Nature Communications*, *6*(6809), 1–8. https://doi.org/10.1038/ncomms7809

Vogel, H., Rosén, P., Wagner, B., Melles, M., & Persson, P. (2008). Fourier transform infrared spectroscopy, a new cost-effective tool for quantitative analysis of biogeochemical properties in long sediment records. *Journal of Paleolimnology*, *40*(2), 689–702. https://doi.org/10.1007/s10933-008-9193-7

von Blanckenburg, F., Belshaw, N. S., & O'Nions, R. K. (1996). Separation of 9Be and cosmogenic 10Be from environmental materials and SIMS isotope dilution analysis. *Chemical Geology*, *129*(1–2), 93–99. https://doi.org/10.1016/0009-2541(95)00157-3

Walker, M. D., Wahren, C. H., Hollister, R. D., Henry, G. H. R., Ahlquist, L. E., Alatalo, J. M., … Wookey, P. A. (2006). Plant community responses to experimental warming across the tundra biome. *Proceedings of the National Academy of Sciences of the United States of America*, *103*(5), 1342–1346. https://doi.org/10.1073/pnas.0503198103

Weijers, J. W. H., Schouten, S., van den Donker, J. C., Hopmans, E. C., & Sinninghe Damsté, J. S. (2007). Environmental controls on bacterial tetraether membrane lipid distribution in soils. *Geochimica et Cosmochimica Acta*, *71*(3), 703–713. https://doi.org/10.1016/j.gca.2006.10.003

Young, N. E., Schaefer, J. M., Briner, J. P., & Goehring, B. M. (2013). A 10Be production-rate calibration for the Arctic. *Journal of Quaternary Science*, *28*(5), 515–526. https://doi.org/10.1002/jqs.2642

Zamin, T. J., & Grogan, P. (2012). Birch shrub growth in the low Arctic: The relative importance of experimental warming, enhanced nutrient availability, snow depth and caribou exclusion. *Environmental Research Letters*, *7*, 034027. https://doi.org/10.1088/1748-9326/7/3/034027

Zink, K. G., Vandergoes, M. J., Mangelsdorf, K., Dieffenbacher-Krall, A. C., & Schwark, L. (2010). Application of bacterial glycerol dialkyl

glycerol tetraethers (GDGTs) to develop modern and past temperature estimates from New Zealand lakes. *Organic Geochemistry*, *41*(9), 1060–1066. https://doi.org/10.1016/j.orggeochem.2010.03.004

SUPPORTING INFORMATION

Additional supporting information may be found online in the Supporting Information section at the end of the article.

How to cite this article: Crump SE, Miller GH, Power M, et al. Arctic shrub colonization lagged peak postglacial warmth: Molecular evidence in lake sediment from Arctic Canada. *Glob Change Biol*. 2019;00:1–13. https://doi.org/10.1111/gcb.14836